NUCL SCI TECH (2017) 28:149
DOI 10.1007/s41365-017-0302-z

Thermal–hydraulic performance analysis of a subchannel with square and triangle fuel rod arrangements using the entropy generation approach

S. Talebi[1] · M. M. Valoujerdi[1]

Received: 14 September 2016 / Revised: 30 December 2016 / Accepted: 31 December 2016 / Published online: 8 September 2017

Abstract The present paper discusses entropy generation in fully developed turbulent flows through a subchannel, arranged in square and triangle arrays. Entropy generation is due to contribution of both heat transfer and pressure drop. Our main objective is to study the effect of key parameters such as spacer grid, fuel rod power distribution, Reynolds number *Re*, dimensionless heat power ω, length-to-fuel-diameter ratio λ, and pitch-to-diameter ratio ξ on subchannel entropy generation. The analysis explicitly shows the contribution of heat transfer and pressure drop to the total entropy generation. An analytical formulation is introduced to total entropy generation for situations with uniform and sinusoidal rod power distribution. It is concluded that power distribution affects entropy generation. A smoother power profile leads to less entropy generation. The entropy generation of square rod array bundles is more efficient than that of triangular rod arrays, and spacer grids generate more entropy.

Keywords Entropy generation · Rod bundles · Thermal–hydraulics · Spacer grids

✉ S. Talebi
sa.talebi@aut.ac.ir

[1] Department of Energy Engineering and Physics, Amirkabir University of Technology, 424 Hafez Avenue, P.O. Box 15875-4413, Tehran, Iran

1 Introduction

High heat transfer performance is vital in many engineering heat transfer applications such as heat exchangers and nuclear power plants. The common methods to increase the heat transfer rate in a thermal system (the surface exchange or the increase in coolant velocity) may lead to either an increase in thermal system dimensions, or an increase in system pressure drop. For design of thermal equipment, both heat transfer rate and pressure drop must be considered.

Irreversibility in thermal equipment can be caused by heat transfer between heated walls and the surrounding coolant (of finite temperature gradient) and the fluid's viscous effect. Irreversibility causes generation of entropy in thermodynamic systems. Irreversibilities, caused by heat transfer and pressure drop, compete with each other and attempt to reduce entropy generation associated with heat transfer, and vice versa.

Because the entropy generation is a direct measure of the irreversibilities associated with heat transfer and pressure drop, the thermal system performance can be improved by minimizing the total entropy generation of the convective heat transfer process. Many authors have focused on the entropy generation of a single-phase flow in various ducts. Bejan [1] proposed an optimum Reynolds number for pipe flow leading to the minimum entropy generation rate under fixed heat duty and flow rate and reviewed on the thermodynamic optimization (or entropy generation minimization) of flow geometry in single-phase engineering flow systems [2]. Sarangi and Chowdhury [3] analysed entropy generation in a counter flow heat exchanger and derived expressions in terms of non-dimensional parameters. The thermodynamic optimization

method for tree-shaped flow geometries during single-phase flow was proposed by Zimparov et al. [4], by assuming a laminar and fully developed flow and developing analytical equations to determine the entropy generation in these geometries. Sahin [5–7] analysed the entropy generation in both laminar and turbulent single-phase fluid flows through a duct with a constant heat flux condition and investigated the entropy generation for a fully developed turbulent fluid flow in a smooth duct subjected to constant wall temperature. Temperature dependence of the viscosity was taken into consideration in the analysis. The ratio of the pumping power to the total heat flux decreased considerably when fluid was heated and the entropy generation per unit heat flux reached a minimum along the duct length for viscous fluids.

Jankowski [8] presented a method to minimize entropy generation by adjusting the duct's cross section to control the competing fluid flow and heat transfer irreversibilities, so as to minimize the total entropy generation rate. Given the flow rate, heat transfer rate, available cross-sectional area, and the fluid properties, a general design correlation was proposed to determine the optimal shape of a duct in a single-phase condition. Jarungthammachote [9] analysed entropy generation of a fully developed single-phase laminar flow in a hexagonal duct at constant heat flux. Water and engine oil were used to study the fluid effect on the entropy generation. The aspect ratio of a hexagonal duct was investigated to show its effect on the entropy generation. The entropy generations calculated with ducts, of different cross sections, but in the same hydraulic diameter and cross-sectional area, showed that the rectangular duct was of the highest entropy generation, while the circular was of the least. Other authors developed theories on entropy generation for two-phase flow in ducts [10–13].

Entropy generation approach has been used in the nuclear reactor technology. Talebi [14] studied effects of thermal hydraulic on entropy generation in a vertical boiling channel using drift flux void fraction model and found that power distribution affected directly total entropy generation for uniform distribution. Goudarzi and Talebi [15, 16] minimized entropy generation for both single and two phase of natural circulation loops. Using the second law of thermodynamic analysis for a fuel element, Poddar et al. [17] found optimum points for different wall heat fluxes in low Reynolds number. In their study on applicability of entropy generation minimization for various thermodynamic processes, Cheng and Liang [18] reported that entropy generation minimization led to maximum output power. Poddar et al. [19] studied a entropy generation in a rod bundle and investigated geometrical effects on thermodynamic performance of a rod bundle.

The effect of spacer grids and fuel rod power distribution has not been investigated yet. Spacer grids are fixed in several positions along the fuel assembly axial length. Spacer grids lead to more pressure drop along fuel assembly and more heat removal by convection heat transfer from cladding outer surface. Generally, entropy generation analysis tool can determine the extent to which each parameter affects the entropy generation and consequently the efficiency of the system. Based on these predictions and economic issues, a final decision can be made to choose the most appropriate design parameters.

The main objective of this paper is to investigate the thermodynamic performance of a subchannel with triangle and square arrangements. Entropy generation method is used to study the effect of important parameters such as spacer grid, fuel rod power distribution, Reynolds number Re, dimensionless heat power ω, length-to-fuel-diameter ratio λ, and pitch-to-diameter ratio ξ.

2 Mathematical model

A correlation for entropy generation in a subchannel with square and triangle rod arrays was derived. As shown in Fig. 1a, D is the rod diameter and P is centre-to-centre distance of two adjacent rods. This study is concerned with the entropy generation in the interior subchannels, but the development of an expression for the side and corner subchannels is analogous to the interior subchannel. Flow conditions are representative of those of PWRs.

Assuming that the kinetic and potential energies are much less than the thermal energy component, the steady-state energy equation for the control volume with a length of dz (Fig. 1b) is given by

$$\mathrm{d}T/\mathrm{d}z = q''\Pi_{\mathrm{w}}/\left(AGC_{\mathrm{p}}\right), \tag{1}$$

where T is the coolant temperature, Π_{w} is the wetted perimeter, A is the channel flow area, G is the mass flux, C_{p} is the coolant specific heat at constant pressure, and q'' is induced surface heat flux defined as

$$q'' = Q_{\mathrm{sc}}/(\Pi_{\mathrm{w}}L) \text{ for uniform heat flux,} \tag{2a}$$

$$q'' = \pi Q_{\mathrm{sc}}/(2\Pi_{\mathrm{w}}L)\sin(\pi x/L) \text{ for sinusoidal heat flux,} \tag{2b}$$

where Q_{sc} is the heat added to the coolant flowing through the subchannel, L is subchannel length, and x is axial distance from the geometrical beginning of the fuel rod. The total entropy generation within the control volume shown in Fig. 1b is:

$$\mathrm{d}S_{\mathrm{ep}} = AG\mathrm{d}S - q''\Pi_{\mathrm{w}}\mathrm{d}z/T_{\mathrm{w}}, \tag{3}$$

where $\mathrm{d}S_{\mathrm{ep}}$ is the entropy generation and T_{w} is the local rod surface temperature. dS is the change of specific entropy for an incompressible fluid and can be calculated from:

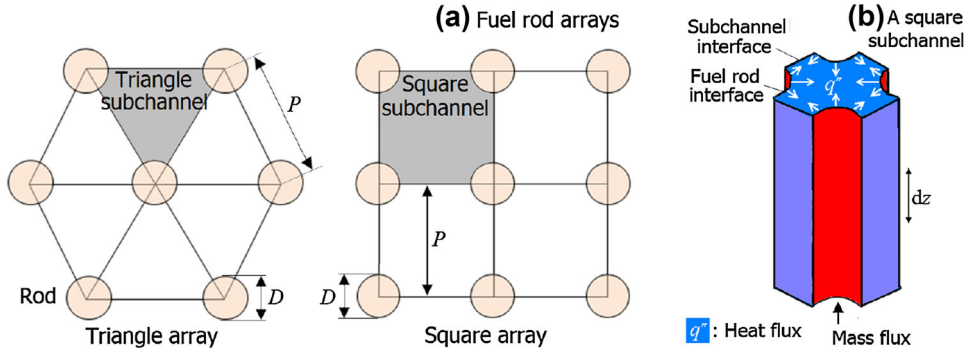

Fig. 1 (Colour online) Schematics of the rod arrays (**a**) and a single square subchannel (**b**)

$$dI = C_p dT = T dS + dp/\rho, \quad dS = \left[C_p dT - dp/\rho\right]/T, \quad (4)$$

where I is the specific enthalpy, p is the pressure, and ρ is the coolant density. The rod surface temperature is obtained by:

$$\begin{aligned} &T_w = T + \Delta T; \quad \Delta T = q''/h; \quad h = kNu/D_{hy}; \\ &D_{hy} = 4A/\Pi_w, \\ &\Pi_w = \pi P, A = D^2 - \pi P^2/4 \text{ for square array}; \\ &\Pi_w = \pi P/2, \\ &A = 3^{1/3}D^2/4 - \pi P^2/8 \text{ for triangle array}, \end{aligned} \quad (5)$$

where h is the heat transfer coefficient, Nu is the Nusselt number, k is the coolant thermal conductivity, and D_{hy} is the channel hydraulic diameter. Thus, we have

$$\frac{dS_{ep}}{dz} = \frac{q''\Pi_w \Delta T}{T^2(1 + \Delta T/T)} + \frac{GA}{\rho T} - \frac{dp}{dz}. \quad (6)$$

In Eq. (6), $\Delta T/T$ is very small and can be neglected. The pressure gradient term can be given by:

$$-\frac{dp}{dz} = \underbrace{\frac{fG^2}{2\rho D_{hy}}}_{\text{Friction}} + \underbrace{\rho g}_{\text{Gravity}} + \underbrace{G^2 \frac{d(1/\rho)}{dz}}_{\text{Acceleration}}, \quad (7)$$

where f is the friction factor. Acceleration pressure drop has the lowest contribution to total pressure drop and can be neglected. Substituting Eq. (7) into Eq. (6) and simplifying:

$$\frac{dS_{ep}}{dz} = \underbrace{\frac{4q''^2 A}{T^2 Nuk}}_{\text{Heat transfer}} + \underbrace{\left(\frac{fG^3\Pi_w}{8\rho^2} + GAg\right)\frac{1}{T}}_{\text{Pressure drop}}. \quad (8)$$

Geometry parameters in Eq. (8) are channel flow area and wetted perimeter. Therefore, Eq. (8) can be used for both square and triangle rod array subchannels using Eq. (6) to determine the flow area and the wetted perimeter.

Todreas and Kazimi [20] showed that friction factor and Nusselt number for non-circular (especially rod array) geometries could not be obtained by circular tube correlations using the equivalent hydraulic diameter concept. Also, for the fully developed turbulent flow through rod bundles, Nu values may significantly deviate from the circular geometry due to strong geometric non-uniformity of the subchannels. For a bare rod bundle array, friction factor (f) and Nusselt number are functions of Reynolds number (Re) and pitch-to-diameter ratio ($\xi = P/D$) [14]:

$$f = C_f/Re^{0.18} = \left[a + b(\xi - 1) + c(\xi - 1)^2\right]/Re^{0.18}, \quad (9)$$

$$Nu = Nu_\infty/\Phi = 0.023Re^{0.8}Pr^{0.333}/\left[a + b\xi + ce^{d(\xi-1)}\right], \quad (10)$$

where C_f is the rod bundle friction factor, Nu is the Nusselt number for rod array geometry, Nu_∞ is the Nusselt number for a circular channel with an equivalent hydraulic diameter, and Pr is the Prandtl number. Coefficients in Eqs. (9) and (10) for fully developed turbulent flow through rectangle and triangle arrays are given in Table 1 [20].

For considering grid spacer effect on heat transfer, Miller et al. [21] proposed the following correlation:

$$Nu/Nu_{in} = 1 + 465.4Re^{-0.5}\varepsilon^2 \exp\left(-7.31 \times 10^{-6}Re^{1.15}z/D_{hy}\right), \quad (11)$$

where Nu_{in} is Nusselt number for array geometry without considering grid spacer effect, $\varepsilon = 0.233$ is blockage ratio, and z is the grid spacer distance.

For evaluation of total entropy generation in the subchannel, Eq. (8) must be integrated from subchannel inlet into outlet. This can be done analytically for uniform heat flux along the subchannel, following Jarungthammachote [9]. For uniform and sinusoidal heat flux, the local coolant temperature can be obtained by integrating Eq. (1) as follows:

$$\begin{aligned} &T = T_{in} + Q_{sc}z/\left(ALGC_p\right) \text{ for uniform heat flux}, \\ &T = T_{in} + Q_{sc}[1 - \cos(\pi z/L)]/\left(ALGC_p\right) \\ &\quad \text{for sinusoidal heat flux}. \end{aligned} \quad (12)$$

Table 1 Coefficients in Eqs. (9) and (10) for rod bundle friction factor in square and triangle rod arrays

Rod arrays	Equation (9), $1.0 \le P/D \le 1.1$			Equation (9), $1.1 < P/D \le 1.5$			Equation (10), $1.5 < P/D \le 1.9$			
	A	B	C	A	B	C	A	B	C	D
Square array	0.09423	0.5806	−1.239	0.1339	0.09059	−0.09956	0.9217	0.1478	−0.1130	−7
Triangle array	0.09378	1.398	−8.664	0.1458	0.03632	−0.03333	0.9090	0.0783	−0.1283	2.4

2.1 Uniform heat flux without spacer grid

By substituting Eq. (12) into Eq. (8) and integrating by analytical method, the total entropy generation (S_{gen}) can be obtained:

$$S_{gen} = \frac{4AQ_{sc}^2}{LkNu\Pi_w^2 T_{in}T_{out}} + \left(\frac{G^3\Pi_w Lf}{8\rho^2} + GALg\right)\frac{\ln(T_{out}/T_{in})}{T_{out}-T_{in}}, \quad (13)$$

where L is the subchannel length, and the heat added to the coolant flowing through the subchannel equals to the total power of one rod ($Q_{sc} = Q_R$) for square array, and $Q_{sc} = Q_R/2$ for triangle array.

2.2 Sinusoidal heat flux with spacer grid

In order to calculate entropy generation by heat transfer for non-uniform (sinusoidal) heat flux, Eqs. (11) and (12) substitute into Eq. (8) and then integrating by numerical methods. For simplicity, integrating intervals are assumed to be equal to distance of two consecutive spacer grid. It should be noted because the dimension of each spacer grid is significantly lower than the hydraulic diameter of channel, the heat transfer effect of any spacer grid on the next one is not considered. Following shah and Sekulic [22], entropy generation by fluid friction under non-adiabatic conditions for a incompressible fluid can be calculated. So the total entropy generation can be written:

$$S_{gen} = \sum_{0}^{n_0-1}\left[\int_{n\mathrm{d}z}^{(n+1)\mathrm{d}z} AB\,\mathrm{d}z\right] + \frac{GA\Delta p}{\rho T_{lm}}, \quad (14)$$

where $n_0 = 15$ is the number of spacer grids, n is the number of axial increment, and dz is the distance between the spacer grids. A, B, Δp, T_{lm}, and q_{max} are written as follows:

$$A = \frac{4A\left[q''_{max}\sin(\pi z/L)\right]^2}{kNu\left(1+465.4Re^{-0.5}\varepsilon^2\exp\left[-7.31\times10^{-6}Re^{1.15}(z-n\mathrm{d}z)/D_{hy}\right]\right)}$$

$$B = \left(T_{in} + \frac{q''_{max}\Pi_w L}{\pi AGC_p}\left[1-\cos(\pi z/L)\right]\right)^{-1}$$

$$\Delta p = \left(\frac{fL}{D_{hy}} + n_0K_f\right)\frac{G^2}{2p} + \rho gL$$

$$T_{lm} = \frac{\ln(T_{out}/T_{in})}{T_{out}-T_{in}}$$

$$q''_{max} = \frac{\pi Q_{sc}}{2\Pi_w L}$$

where $K_f = 0.242$ is local loss coefficient for each spacer grid [23].

It is often customary to use the entropy generation in dimensionless form [9]: Ψ_T = Total entropy generation·$(T_{out}-T_{out})/Q_{sc}$, Ψ_H = Heat transfer entropy generation·$(T_{out}-T_{out})/Q_{sc}$, and Ψ_P = Pressure drop entropy generation·$(T_{out}-T_{out})/Q_{sc}$; where Ψ_T, Ψ_H, and Ψ_P are total, heat transfer, and pressure drop dimensionless entropy generation, respectively.

We note that the present analysis is valid only for the single-phase conditions. The minimum wall temperature for bubble formation on the rod surface can be calculated by [24]:

$$T_{ONB} = T_{sat} + 0.556\left(\frac{q''}{1082\,p^{1.156}}\right)^{0.463\,p^{0.0234}}, \quad (15)$$

where p is in bar and q'' is in W/m^2. The thermal–hydraulic and geometry design parameters of subchannels, shown in Fig. 1, should be selected in order not to violate Eq. (15).

3 Results and discussion

Equations (13) and (14) were used to minimize entropy generation in a vertical subchannel for both square and triangle rod arrays. Effects of Reynolds number Re, dimensionless heat power ω, length-to-fuel-diameter ratio λ, and pitch-to-diameter ratio ξ, which are important for thermal–hydraulic performance of a subchannel, were analysed. Entropy generation in subchannels with square and triangle arrays under different conditions was compared for uniform heat flux without considering grid spacers effects; and for sinusoidal heat flux with grid spacers. Figure 2a, b shows dimensionless entropy generation verse Re for square and triangle subchannel, for the entropy generation due to heat transfer (ψ_H) and pressure drop (ψ_P), and total entropy generation (ψ_T), under uniform heat flux and without considering grid spacer influence; while Fig. 2c, d represents for sinusoidal heat flux with considering grid spacer effect. As illustrated, the ψ_P contribution to ψ_T is rather insignificant, whereas the ψ_H heat transfer contributions dominate due to large value of heat flux. Also Fig. 2 shows that for constant parameters, the entropy generation decreases with increasing Re, as the heat transfer coefficient increases with Re and this causes

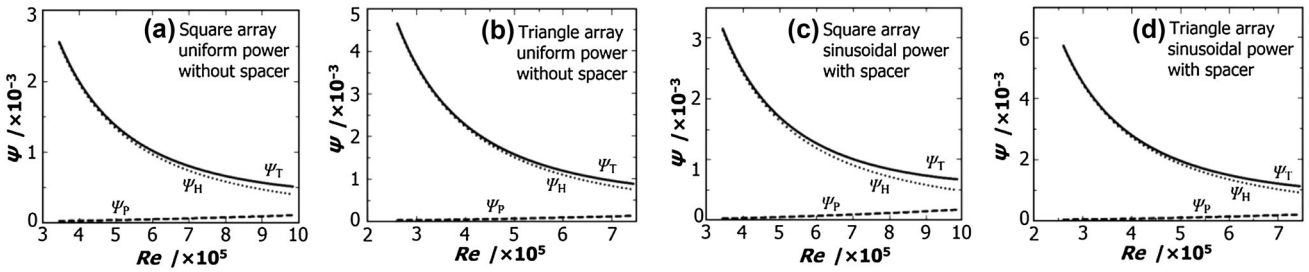

Fig. 2 Dimensionless entropy generation versus *Re* number for square (**a**) and triangle (**b**) arrays in uniform power without spacer, and for square (**c**) and triangle (**d**) arrays in sinusoidal power with spacer. $L = 4$ m, $D_F = 0.0095$ m, $\xi = 1.32$, $P = 15.5$ MPa, $T_{in} = 286$ °C, and $Q_R = 64.4$ kW

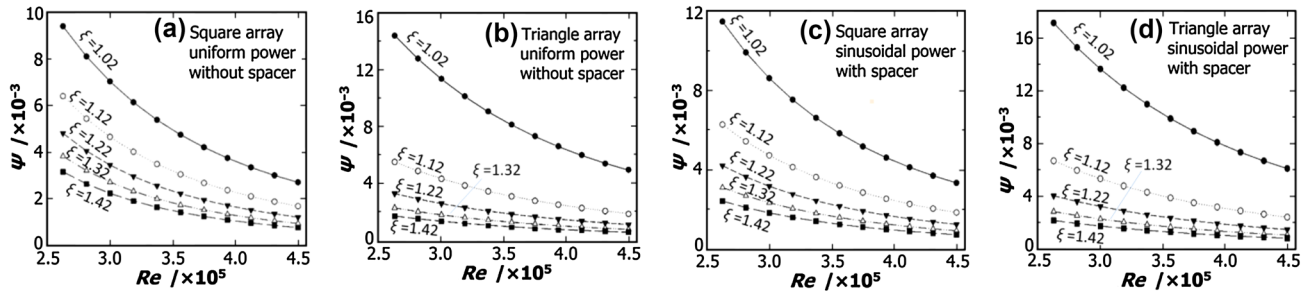

Fig. 3 Dimensionless entropy generation versus *Re* at various ξ ratios, for square (**a**) and triangle (**b**) arrays in uniform power without spacer, and for square (**c**) and triangle (**d**) arrays in sinusoidal power with spacer. $L = 4$ m, $D_F = 0.0095$ m, $P = 15.5$ MPa, $T_{in} = 286$ °–C, and $G = 3530$ kg/m^{2}s

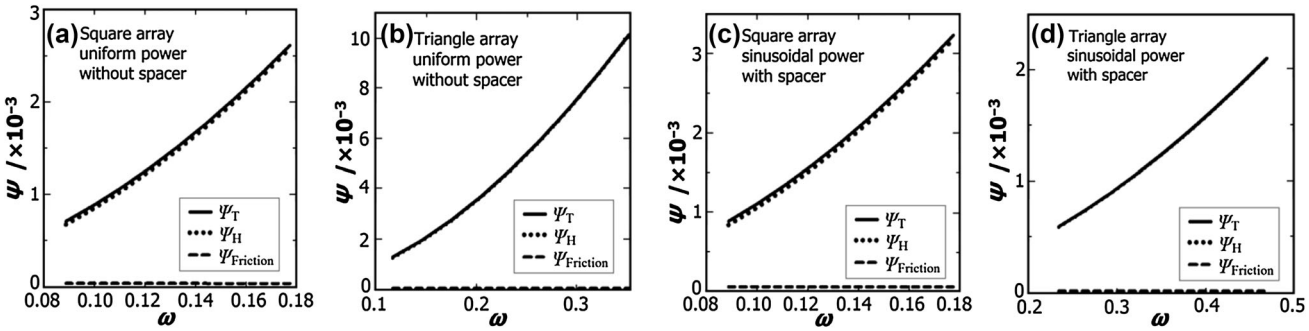

Fig. 4 Entropy generation versus dimensionless heat power ω for square (**a**) and triangle (**b**) arrays in uniform power without spacer, and for square (**c**) and triangle (**d**) arrays in sinusoidal power with spacer. $L = 4$ m, $D_F = 0.0095$ m, $\xi = 1.32$, $P = 15.5$ MPa, $T_{in} = 286$ °C, and $G = 3530$ kg/m^{2}s

the heat transfer to occur at a lower temperature difference in the wall–bulk; hence the reduction in entropy generation. On the other side, the triangular subchannel produces more entropy than the square one.

Figure 3 shows the entropy generation as a function of *Re* for ξ values of 1.02–1.42. Higher ξ increases the subchannel mass flow rate and consequently improves the heat transfer performance, hence the decrease in entropy generation. Figure 3 illustrates comparisons between total entropy generation for square and triangle array subchannels with a fixed heat power, inlet temperature, inlet mass flux, and for various pitch-to-diameter ratios. The entropy generation in triangle array is greater than square ones due to changes in rod diameter. Therefore, in terms of entropy generation, reactors with square fuel array (or PWRs) can perform better than those with triangle fuel array (or VVERs). Even spacer grids and sinusoidal power have identical influence over triangular and square arrays. Figure 3c, d shows slight increase in entropy generation relative to Fig. 3a, b, respectively.

Figure 4 shows the entropy generation as a function of dimensionless heat power ω for the subchannel with square and triangle rod arrays at $L = 4$ m, $D_F = 0.0095$ m, $\xi = 1.32$, $P = 15.5$ MPa, $T_{in} = 286$ °C, and $G = 3530$ kg/m^{2}s. The entropy generation ψ increases with ω. For a fixed heat transfer coefficient, increasing the

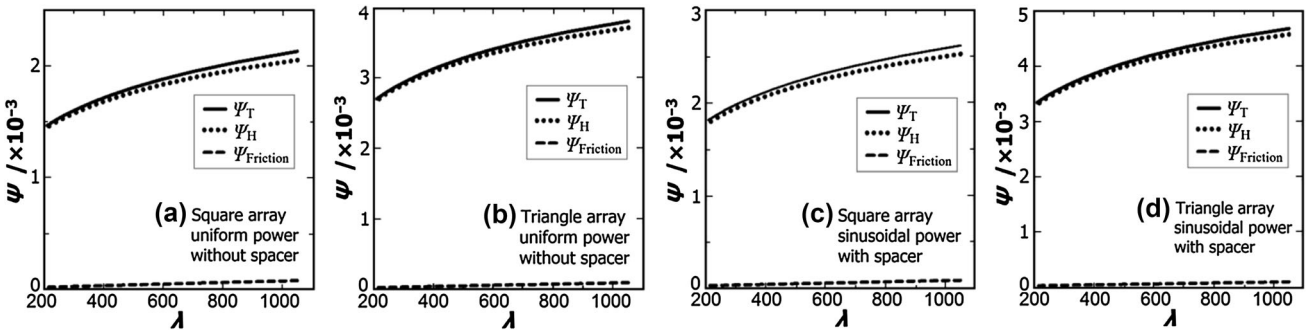

Fig. 5 Dimensionless entropy generation versus length-to-diameter ratio λ for square (**a**) and triangle (**b**) arrays in uniform power without spacer, and for square (**c**) and triangle (**d**) arrays in sinusoidal power with spacer. $\xi = 1.32$, $P = 15.5$ MPa, $T_{in} = 286$ °C, $Q_R = 64.4$ kW, and $G = 3530$ kg/m^{2}s

heat power leads to a higher wall–bulk temperature difference, hence the increase in entropy generation. According to Eq. (7), entropy generation number is proportional to heat power, thus entropy generation increases. As expected, friction pressure drop contributions are insignificant.

Figure 5 represents dimensionless entropy generation ψ as a function of the length-to-diameter ratio λ, at $\xi = 1.32$, $P = 15.5$ MPa, $T_{in} = 286$ °C, $Q_R = 64.4$ kW, and $G = 3530$ kg/m^{2}s. This constraint causes that length and fuel rod diameter compensate each other, as an increase in length means a relative decrease in fuel rod diameter, and a greater λ increases entropy generation. Comparing Fig. 5a with Fig. 5c, the spacer grid leads to slight increase in entropy generation. However, the role of sinusoidal heat power cannot be ignored for entropy generation growth. Again, applying spacer grid leads to more entropy generation for both triangle and square arrays (Fig. 5c, d).

The effects of channel power profile and spacer grid on the total dimensionless entropy generation ψ as a function of *Re* are demonstrated in Fig. 6. It can be seen that situations according to uniform power profile with and without spacer grid generate approximately identical entropy for lower *Re*, while for larger *Re*, uniform power with grid spacer produces more entropy. This fact is extendible for sinusoidal profile, situations with and without spacer grid and close to $Re = 5 \times 10^5$ have approximately identical entropy generation, while after this critical value the case with spacer grid begins to over taking. Also uniform power distribution generates less entropy due to lower wall–bulk temperature difference than the sinusoidal power distribution.

Therefore, flattened neutronic flux and consequently uniform power distribution in PWRs or VVERs cores not only widens the safety margin but also leads to better thermal–hydraulic performance associated with the entropy generation.

4 Conclusion

Less entropy generation during cooling of a reactor core leads to increased thermal–hydraulic efficiency. An analytical study has been performed to investigate the entropy generation for a single-phase and fully developed turbulent viscous flow in a single channel with square and triangle arrays. An interior subchannel of a rod bundle is selected as a representative of LWR for this analysis, and the selected key thermal–hydraulic parameters and channel geometry are in the range of PWRs. The effects of different parameters on the total entropy generation of subchannel are studied. The important results derived from present paper which give further insight into the area of entropy generation in a nuclear reactor core are the following:

1. The two most important phenomena that generate entropy are heat transfer and pressure drop. The contribution of pressure drop to total entropy generation is rather insignificant, compared to that of heat transfer.
2. Increasing the pitch-to-diameter ratio would lead to increase in subchannel mass flow rate and consequently improvement in heat transfer performance, causing the entropy generation number to decrease.
3. The entropy generation decreases with an increase in the Reynolds number and vice versa.
4. For a fixed heat transfer coefficient increasing the heat power would lead to heat being transferred at a higher wall–bulk temperature difference, causing the entropy generation to increase.
5. An increase in channel length or fuel rod diameter leads to more entropy generation.
6. Entropy generation in reactors with triangle rod arrays is greater than those with square arrays.
7. Power distribution profile has an important effect on entropy generation in a reactor core. A smoother power profile leads to lower entropy generation and better thermal efficiency.

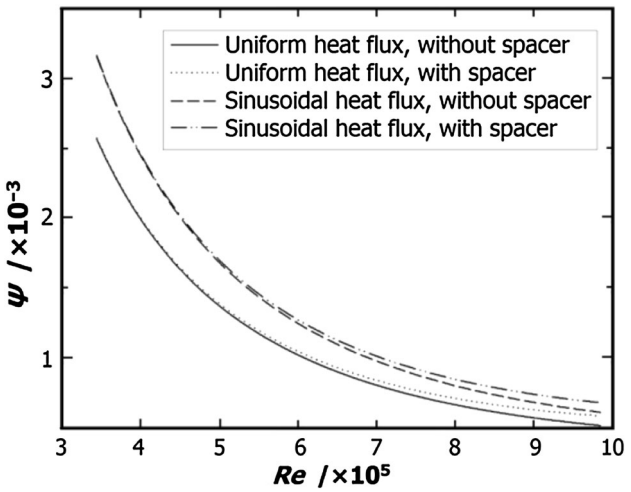

Fig. 6 Total dimensionless entropy generation for uniform and sinusoidal and spacer grid $L = 4$ m, $D_F = 0.0095$ m, $\xi = 1.32$, $P = 15.5$ MPa, G = 3530 kg/m^{2}s, and $T_{in} = 286$ °C

8. Spacer grids lead to increase in entropy generation in the channel.
9. Generally, entropy generation analysis tool can help designers to determine the extent to which each parameter affects the entropy generation and consequently the efficiency of the system. Based on these predictions and economic issues, the designer will make a final decision to choose the most appropriate design parameters.

References

1. A. Bejan, Second law analysis in heat transfer. Energy **5**, 721–732 (1980). doi:10.1016/0360-5442(80)90091-2
2. A. Bejan, Thermodynamic optimization of geometry in engineering flow systems. Int. J. Exergy **4**, 269–277 (2001). doi:10.1016/S1164-0235(01)00028-0
3. S. Sarangi, K. Chowdhury, On the generation of entropy in a counter flow heat exchanger. Cryogenics **22**, 63–65 (1982). doi:10.1016/0011-2275(82)90095-9
4. V.D. Zimparov, A.K. Silva, A. Bejan, Thermodynamic optimization of tree-shaped flow geometries. Int. J. Heat Mass Transf. **49**, 1619–1630 (2006). doi:10.1016/j.ijheatmasstransfer.2005.11.016
5. A.Z. Sahin, Thermodynamics of laminar viscous flow through a duct subjected to constant heat flux. Energy **21**, 1179–1187 (1996). doi:10.1016/0360-5442(96)00062-X
6. A.Z. Sahin, Entropy generation and pumping power in a turbulent fluid flow through a smooth pipe subjected to constant heat flux. Int. J. Exergy **2**, 314–321 (2002). doi:10.1016/S1164-0235(02)00082-1
7. A.Z. Sahin, Entropy generation in turbulent liquid flow through a smooth duct subjected to constant wall temperature. Int. J. Heat Mass Transf. **43**, 1469–1478 (2000). doi:10.1016/S0017-9310(99),00216-1
8. T.A. Jankowski, Minimizing entropy generation in internal flows by adjusting the shape of the cross-section. Int. J. Heat Mass Transf. **52**, 3439–3445 (2009). doi:10.1016/j.ijheatmasstransfer.2009.03.016
9. S. Jarungthammachote, Entropy generation analysis for fully developed laminar convection in hexagonal duct subjected to constant heat flux. Energy **35**, 5374–5379 (2010). doi:10.1016/j.energy.2010.07.020
10. F.J. Collado, The law of stable equilibrium and the entropy-based boiling curve for flow boiling. Energy **30**, 807–819 (2005). doi:10.1016/j.energy.2004.04.007
11. D. Rakshit, R. Narayanaswamy, K.P. Thiagarajan, Estimation of entropy generation by heat transfer from a liquid in an enclosure to ambient. Anziam J. **51**, 852–873 (2011). doi:10.21914/anziamj.v51i0.2618
12. R. Revellin, S. Lips, S. Khandekar et al., Local entropy generation for saturated two-phase flow. Energy **34**, 1113–1121 (2009). doi:10.1016/j.energy.2009.03.014
13. R. Revellin, J. Bonjour, Entropy generation during flow boiling of pure refrigerant and Refrigerant-oil mixture. Int. J. Refrig. **34**, 1040–1047 (2011). doi:10.1016/j.ijrefrig.2011.01.010
14. S. Talebi, Effect of thermal–hydraulic parameters on entropy generation in a boiling channel. Multiph. Sci. Technol. **4**, 287–303 (2014). doi:10.1615/MultScienTechn.v26.i4.20
15. N. Goudarzi, S. Talebi, An approach to stability analysis and entropy generation minimization in the single-phase natural circulation loops. Energy **80**, 213–226 (2015). doi:10.1016/j.energy.2014.11.064
16. N. Goudarzi, S. Talebi, Improving performance of two-phase natural circulation loops by reducing of entropy generation. Energy **93**, 882–899 (2015). doi:10.1016/j.energy.2015.09.101
17. A. Poddar, R. Chatterjee, A. Chakravarty et al., Thermodynamic analysis of a solid nuclear fuel element surrounded by flow of coolant through a concentric annular channel. Prog. Nucl. Energy **85**, 178–191 (2015). doi:10.1016/j.pnucene.2015.06.018
18. X. Cheng, X.G. Liang, Discussion on the applicability of entropy generation minimization to the analyses and optimizations of thermodynamic processes. Energy Convers. Manag. **73**, 121–127 (2013). doi:10.1016/j.enconman.2013.04.012
19. A. Poddar, R. Chatterjee, K. Ghosh et al., Performance assessment of longitudinal flow through rod bundle arrangements using entropy generation minimization approach. Energy Convers. Manag. **99**, 359–373 (2015). doi:10.1016/j.enconman.2015.04.075
20. N.E. Todreas, M.S. Kazimi, *Nuclear systems I: Thermal–hydraulic Fundamentals* (Taylor & Francis Group, Abingdon, 2012)
21. D.J. Miller, F.B. Cheung, S.M. Bajorek, On the development of a grid-enhanced single-phase convective heat transfer correlation. Nucl. Eng. Des. **264**, 56–60 (2013). doi:10.1016/j.nucengdes.2012.11.023
22. R. Shah, D. Sekulic, *Fundamentals of the Heat Exchanger Design,* (Wiley, Hoboken, 2003)
23. AEOI, *Final Safety Analysis Report for Bushehr VVER1000 Reactor* (Atomic Energy Organization of Iran, Tehran, 2008)
24. A.E. Bergles, W.M. Rohsenow, The determination of forced-convection surface-boiling heat transfers. J. Heat. Transf T. ASME **86**, 365–371 (1964). doi:10.1115/1.3688697